Acta Cryst E CRYSTALLOGRAPHIC COMMUNICATIONS
ISSN 2056-9890

Crystal structure, Hirshfeld surface analysis and DFT studies of 1,3-bis[2-methoxy-4-(prop-2-en-1-yl)phenoxy]propane

Abdelmaoujoud Taia,[a]* Mohamed Essaber,[a] Tuncer Hökelek,[b] Abdeljalil Aatif,[a] Joel T. Mague,[c] Ali Alsalme[d] and Nabil Al-Zaqri[e]

[a]Laboratory of Molecular Chemistry, Department of Chemistry, Faculty of Sciences Semlalia, University of Cadi Ayyad, PB. 2390, 40001 Marrakech, Morocco, [b]Department of Physics, Hacettepe University, 06800 Beytepe, Ankara, Turkey, [c]Department of Chemistry, Tulane University, New Orleans, LA 70118, USA, [d]Department of Chemistry, College of Science, King Saud University, P.O.Box 2455, Riyadh 11451, Saudi Arabia, and [e]Department of Chemistry, College of Science, King Saud University, PO Box 2455, Riyadh 11451, Saudi Arabia. *Correspondence e-mail: AbdelmaoujoudTaia2018@gmail.com

Received 14 January 2020
Accepted 5 February 2020

Edited by M. Weil, Vienna University of Technology, Austria

Keywords: crystal structure; allyl; methoxyphenoxy; C—H···π(ring); Hirshfeld surface.

Supporting information: this article has supporting information at journals.iucr.org/e

The asymmetric unit of the title compound, $C_{23}H_{28}O_4$, comprises two half-molecules, with the other half of each molecule being completed by the application of twofold rotation symmetry. The two completed molecules both have a V-shaped appearance but differ in their conformations. In the crystal, each independent molecule forms chains extending parallel to the *b* axis with its symmetry-related counterparts through C—H···π(ring) interactions. Hirshfeld surface analysis of the crystal structure indicates that the most important contributions for the crystal packing are from H···H (65.4%), H···C/C···H (21.8%) and H···O/O···H (12.3%) interactions. Optimized structures using density functional theory (DFT) at the B3LYP/6–311 G(d,p) level are compared with the experimentally determined molecular structures in the solid state. The HOMO–LUMO behaviour was elucidated to determine the energy gap.

1. Chemical context

Eugenol (4-allyl-2-methoxyphenol) is the main active constituent of clove oil (75–90%) from various plants (Patra & Saxena, 2010). The 4-allyl-2-methoxyphenol core has several active sites and provides a great responsiveness, making it an excellent precursor in the syntheses of new heterocyclic compounds (Araújo *et al.*, 2010; Xu *et al.*, 2006) and for the development of drugs (Sticht & Smith, 1971). With respect to the biological applications of eugenol 4-allyl-2-methoxyphenol derivatives, it has been shown that these compounds possess potent antimicrobial (Eyambe *et al.*, 2011), antioxidant (Nam & Kim, 2013; Mahapatra *et al.*, 2009; Eyambe *et al.*, 2011), antiviral (Sun *et al.*, 2016), anti-inflammatory (Fonsêca *et al.*, 2016), antidiabetic and anti-leishmania (de Morais *et al.*, 2014) properties. The suppression of melanoma growth caused by eugenol was reported by Ghosh *et al.* (2005), and the ability of eugenol to act as an *in vivo* radio-protective agent was described by Tiku *et al.* (2004). Derivatives of eugenol have also been reported, see, for example: Sadeghian *et al.* (2008); Ma *et al.* (2010).

As a continuation of our research devoted to the study of *o*-alkylation reactions involving eugenol derivatives, we report herein the synthesis, molecular and crystal structures of the title compound, (I). Hirshfeld surface analysis and a density functional theory (DFT) study carried out at the B3LYP/6–

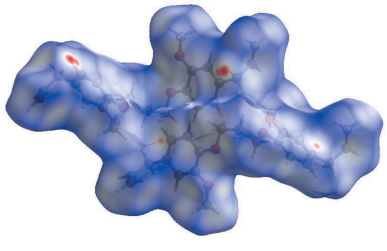

311 G(d,p) level for comparison with the experimentally determined molecular structure.

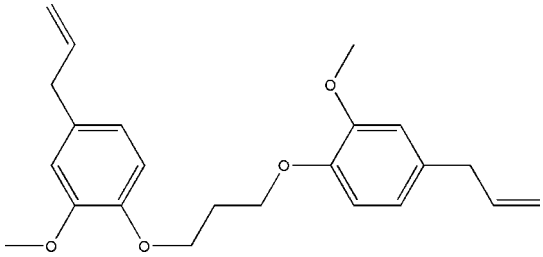

2. Structural commentary

The asymmetric unit of (I) comprises of two half-molecules *A* and *B* that are each completed by twofold rotation symmetry, with the rotation axis running through the central C atom (C8 for molecule *A* and C20 for molecule *B*, respectively) of the propane bridge (Fig. 1). For steric reasons, the exocyclic substituents bound to O1, O2, O3 and O4 are approximately in *trans* positions, with C1—C2—O2—C9, C2—C1—O1—C7, C13—C14—O4—C21 and C14—C13—O3—C19 torsion angles of −167.6 (1), 175.1 (1), 164.6 (1) and −176.7 (1)°, respectively. The two benzene rings in each molecule are nearly perpendicular to each other, with dihedral angles of 86.74 (6)° for *A* (C1–C6) and A^{ii}, and of 88.12 (6) for *B* (C13–C18) and B^{i}, respectively (for symmetry codes, see Fig. 1). The two molecules have a similar V-shaped appearance but different conformations (Fig. 2).

3. Supramolecular features

In the crystal, chains extending parallel to the *b* axis are formed through C7—H7*A*···*Cg*1 (for molecule *A*) and C19—H19*B*···*Cg*2 (for molecule *B*) interactions (Fig. 3, Table 1). Between the chains, only van der Waals contacts occur (Figs. 3 and 4, Table 2).

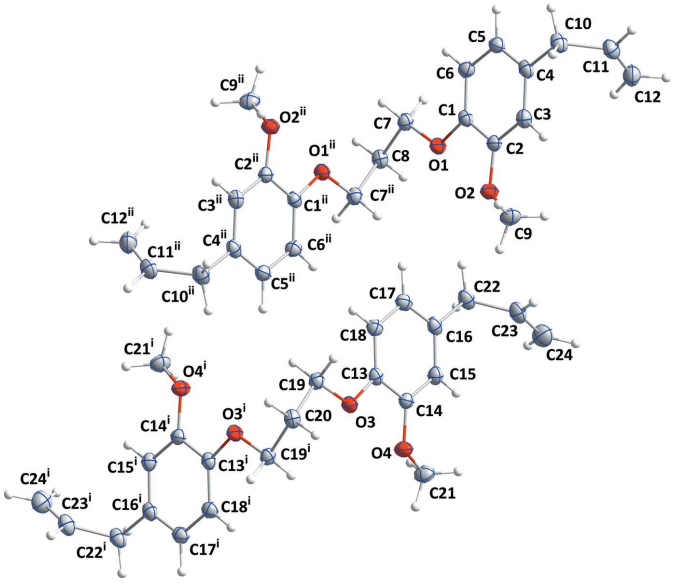

Figure 1
The two independent molecules of (I) with the atom-numbering scheme. Displacement ellipsoids are drawn at the 50% probability level. [Symmetry codes: (i) $-x+\frac{1}{2}, y, -z+\frac{1}{2}$; (ii) $-x+\frac{3}{2}, y, -z+\frac{1}{2}$.]

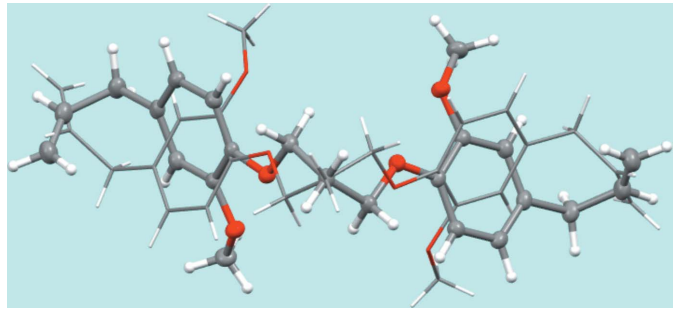

Figure 2
Overlay of the two independent half-molecules, showing their different conformations. Molecule *A* is in light, molecule *B* in dark colours.

4. Hirshfeld surface analysis

In order to quantify the intermolecular interactions in the crystal of (I), a Hirshfeld surface (HS) analysis (Hirshfeld,

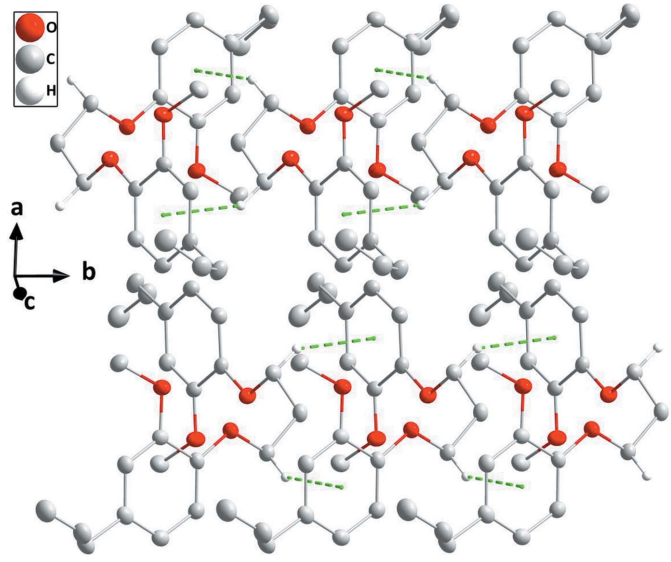

Figure 3
C—H···π(ring) interactions (green dashed lines) enabling the formation of molecular chains extending along the *b*-axis direction.

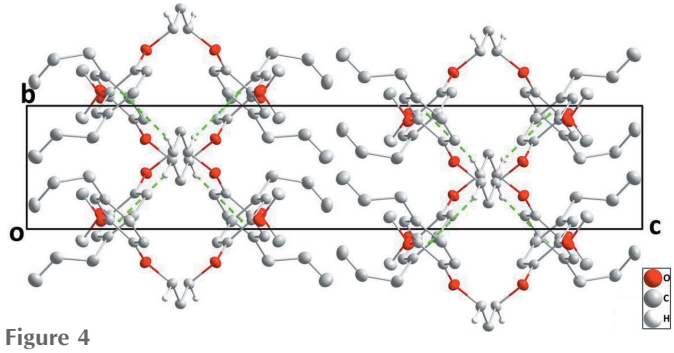

Figure 4
A partial packing diagram viewed along the *a* axis with intermolecular interactions depicted as in Fig. 3.

Table 1
Hydrogen-bond geometry (Å, °).

*Cg*1 and *Cg*2 are the centroids of benzene rings *A* (C1–C6) and *B* (C13–C18), respectively.

D—H···*A*	*D*—H	H···*A*	*D*···*A*	*D*—H···*A*
C7—H7*A*···*Cg*1^{i}	1.003 (16)	2.759 (15)	3.6170 (15)	144.1 (12)
C19—H19*B*···*Cg*2^{v}	0.992 (16)	2.739 (15)	3.5816 (15)	143.0 (11)

Symmetry codes: (i) $x, y-1, z$; (v) $x, y+1, z$.

1977; Spackman & Jayatilaka, 2009) was carried out using *Crystal Explorer 17.5* (Turner *et al.*, 2017). In the HS plotted over d_{norm} (Fig. 5), the white surface indicates contacts with distances equal to the sum of van der Waals radii, and the red and blue colours indicate distances shorter (in close contact) or longer (distinct contact) than the van der Waals radii, respectively (Venkatesan *et al.*, 2016). The bright-red spots appearing near C16 and hydrogen atom H10*B* indicate their roles as the donor and/or acceptor groups in hydrogen-bonding contacts. The shape-index of the HS is a tool to visualize possible π–π stacking interactions by the appearance of adjacent red and blue triangles. The absence of such triangles suggests that there are no notable π–π interactions in

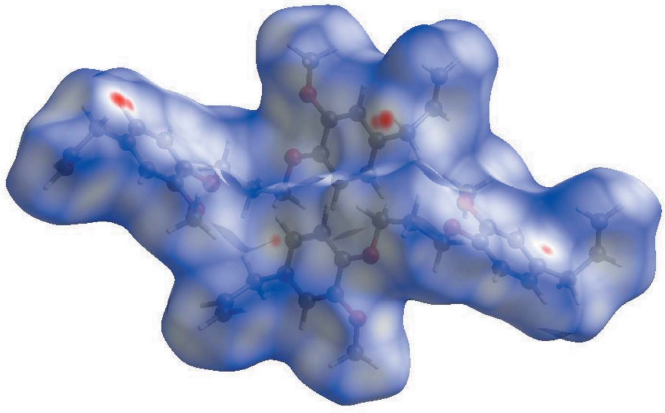

Figure 5
View of the three-dimensional Hirshfeld surface of the title compound plotted over d_{norm} in the range −0.1048 to 1.1789 a.u..

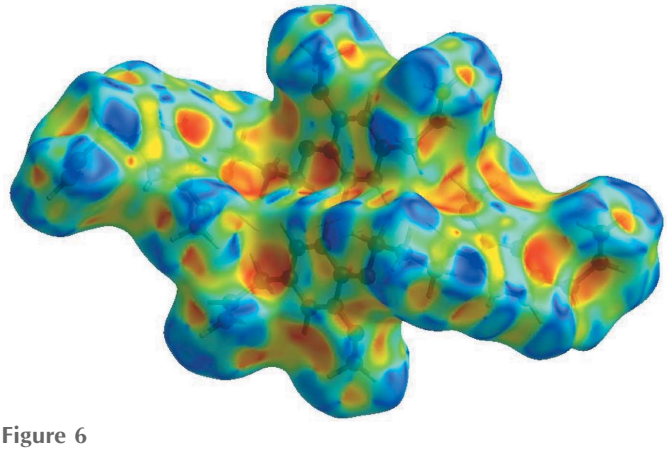

Figure 6
Hirshfeld surface of the title compound plotted over shape-index.

Table 2
Selected interatomic distances (Å).

O1···O2	2.5827 (13)	C14···H20*B*^{i}	2.918 (15)
O2···O1	2.5827 (13)	C15···H21*A*	2.768 (17)
O3···O4	2.5885 (13)	C15···H21*C*	2.784 (17)
O4···O3	2.5885 (13)	C17···H22*A*^{v}	2.727 (19)
O1···H9*C*^{i}	2.736 (18)	C18···H22*A*^{v}	2.764 (18)
O1···H7*B*^{ii}	2.618 (16)	C18···H19*A*	2.759 (15)
O2···H12*A*^{iii}	2.831 (18)	C18···H19*B*	2.739 (15)
O2···H22*B*	2.647 (17)	C19···H18	2.514 (16)
O2···H8*B*^{iv}	2.676 (15)	C21···H15	2.501 (16)
O3···H21*A*^{v}	2.739 (15)	C23···H15	2.862 (16)
O3···H19*A*^{vi}	2.604 (16)	H3···H9*C*	2.33 (2)
O4···H24*B*^{vii}	2.89 (2)	H3···H9*A*	2.29 (2)
O4···H20*B*^{i}	2.732 (15)	H5···H10*A*	2.37 (2)
C2···C7^{v}	3.533 (2)	H6···H7*A*	2.24 (2)
C3···C12	3.282 (2)	H6···H7*B*	2.37 (2)
C6···C10^{i}	3.582 (2)	H6···H18^{viii}	2.50 (2)
C14···C19^{i}	3.555 (2)	H9*A*···H11^{ix}	2.40 (2)
C18···C22^{v}	3.564 (2)	H9*A*···H12*A*^{iii}	2.56 (3)
C2···H8*B*^{iv}	2.914 (16)	H9*B*···H22*A*^{v}	2.52 (2)
C2···H7*A*^{v}	2.971 (15)	H9*B*···H23	2.41 (2)
C3···H9*C*	2.739 (18)	H9*C*···H22*B*^{v}	2.54 (2)
C3···H12*B*	2.783 (19)	H10*A*···H21*A*^{x}	2.58 (2)
C3···H9*A*	2.806 (17)	H12*B*···H12*B*^{iii}	2.55 (3)
C4···H12*B*	2.728 (18)	H15···H21*A*	2.40 (2)
C5···H10*B*^{i}	2.775 (19)	H15···H21*C*	2.26 (2)
C6···H7*A*	2.719 (15)	H17···H22*B*	2.36 (2)
C6···H7*B*	2.786 (15)	H18···H19*A*	2.31 (2)
C6···H10*B*^{i}	2.837 (18)	H18···H19*B*	2.26 (2)
C7···H6	2.529 (16)	H21*C*···H23^{vii}	2.41 (2)
C9···H3	2.492 (16)	H22*A*···H24*A*	2.39 (3)

Symmetry codes: (i) $x, y-1, z$; (ii) $-x+\frac{3}{2}, y, -z+\frac{1}{2}$; (iii) $-x+2, -y, -z+1$; (iv) $-x+\frac{3}{2}, y+1, -z+\frac{1}{2}$; (v) $x, y+1, z$; (vi) $-x+\frac{1}{2}, y, -z+\frac{1}{2}$; (vii) $-x+1, -y, -z+1$; (viii) $-x+\frac{3}{2}, y-1, -z+\frac{1}{2}$; (ix) $-x+2, -y+1, -z+1$; (x) $x+1, y+1, z$.

(I) (Fig. 6). The overall two-dimensional fingerprint plot, Fig. 7*a*, and those delineated into H···H, H···C/C···H and

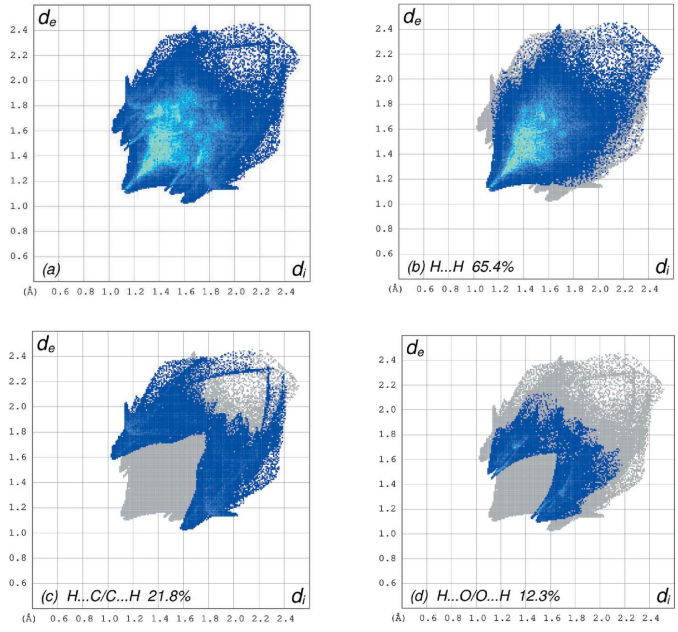

Figure 7
The full two-dimensional fingerprint plots for the title compound, showing (*a*) all interactions, and those delineated into (*b*) H···H, (*c*) H···C/C···H and (*d*) H···O/O···H interactions. The d_i and d_e values are the closest internal and external distances (in Å) from given points on the Hirshfeld surface contacts.

Table 3
Comparison of selected bond lengths and angles (Å, °) in the experinentally determined and computed molecular structures.

Bonds/angles	X-ray (this study)	B3LYP/6–311G(d,p)
O1—C1	1.3704 (15)	1.38958
O1—C7	1.4342 (15)	1.46082
O2—C2	1.3679 (15)	1.39236
O2—C9	1.4280 (16)	1.44976
O3—C13	1.3658 (15)	1.39978
O3—C19	1.4359 (15)	1.47837
O4—C14	1.3697 (15)	1.39894
O4—C21	1.4289 (16)	1.45321
C1—O1—C7	116.96 (10)	118.14221
C2—O2—C9	116.34 (10)	117.63310
C13—O3—C19	116.88 (10)	117.32223
C14—O4—C21	116.03 (10)	117.85841
O1—C1—C6	125.38 (11)	124.87388
O1—C1—C2	115.50 (11)	116.13060
C6—C1—C2	119.12 (11)	118.99394
O2—C2—C3	124.79 (12)	124.29736
O2—C2—C1	115.21 (11)	115.78966

H···O/O···H contacts (McKinnon *et al.*, 2007) are illustrated in Fig. 7*b–d*, respectively, together with their relative contributions to the Hirshfeld surface. The most important intermolecular interactions (Table 2) are H···H contacts, contributing 65.4% to the overall crystal packing, which is reflected in Fig. 7*b* as widely scattered points of high density due to the large hydrogen content of the molecule with the tip at $d_e = d_i = 1.11$ Å. In the presence of C—H···π interactions, pairs of characteristic wings with spikes at the tips at $d_e + d_i =$ 2.62 Å are seen in the fingerprint plot delineated into H···C/C···H contacts, Fig. 7*c* (21.8% contribution to the HS). Finally, the thin and thick pairs of scattered wings in the fingerprint plot delineated into H···O/O···H contacts (12.3% contribution), Fig. 7*d*, have a symmetrical distribution of points with the edges at $d_e + d_i = 2.55$ and 2.58 Å.

Hirshfeld surface representations with the function d_{norm} plotted onto the surface are shown for the H···H, H···C/C···H and H···O/O···H interactions in Fig. 8*a–c*, respectively.

The large number of H···H, H···C/C···H and H···O/O···H intermolecular contacts suggest that these weak interactions play major roles in the crystal packing (Hathwar *et al.*, 2015).

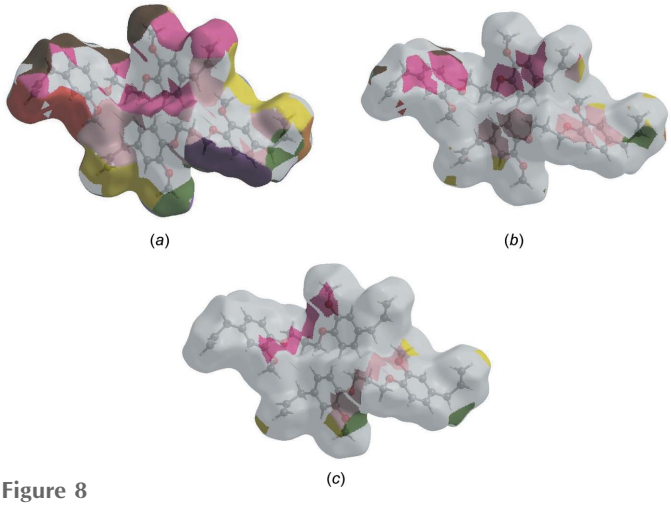

Figure 8
The Hirshfeld surface representations with the function d_{norm} plotted onto the surface for (*a*) H···H, (*b*) H···C/C···H and (*c*) H···O/O···H interactions.

Table 4
Calculated energies and other calculated data for (I).

Total Energy, *TE* (eV)	−32558
E_{HOMO} (eV)	−5.4058
E_{LUMO} (eV)	−0.1807
Gap, ΔE (eV)	5.2251
Dipole moment, μ (Debye)	2.8076
Ionization potential, *I* (eV)	5.4058
Electron affinity, *A*	0.1807
Electronegativity, χ	2.7932
Hardness, η	2.6126
Electrophilicity index, ω	1.4932
Softness, σ	0.3828
Fraction of electrons transferred, ΔN	0.8051

5. DFT calculations

The density functional theory (DFT) optimized molecular structures of (I) were computed in the gas phase on the basis of standard B3LYP functionals and 6–311 G(d,p) basis-set calculations (Becke, 1993) as implemented in *GAUSSIAN 09* (Frisch *et al.*, 2009). The theoretical and experimental results for molecule *A* are in good agreement (Table 3).

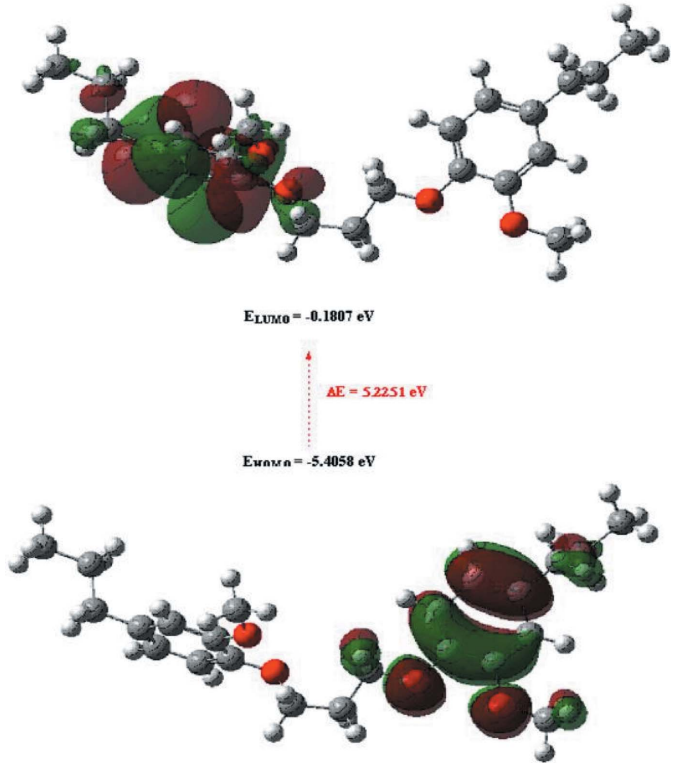

Figure 9
The shapes of HOMO and LUMO orbitals in one of the molecules in (I).

Table 5
Experimental details.

Crystal data	
Chemical formula	$C_{23}H_{28}O_4$
M_r	368.45
Crystal system, space group	Monoclinic, $P2/n$
Temperature (K)	150
a, b, c (Å)	15.4741 (5), 5.0224 (2), 25.5180 (9)
β (°)	99.858 (2)
V (Å^3)	1953.90 (12)
Z	4
Radiation type	Cu $K\alpha$
μ (mm^{-1})	0.68
Crystal size (mm)	0.37 × 0.27 × 0.08
Data collection	
Diffractometer	Bruker D8 VENTURE PHOTON 100 CMOS
Absorption correction	Multi-scan (*SADABS*; Krause *et al.*, 2015)
T_{min}, T_{max}	0.79, 0.95
No. of measured, independent and observed [$I > 2\sigma(I)$] reflections	13935, 3756, 3049
R_{int}	0.033
(sin $\theta/\lambda)_{max}$ (Å^{-1})	0.618
Refinement	
$R[F^2 > 2\sigma(F^2)]$, $wR(F^2)$, S	0.041, 0.109, 1.05
No. of reflections	3756
No. of parameters	358
H-atom treatment	All H-atom parameters refined
$\Delta\rho_{max}$, $\Delta\rho_{min}$ (e Å^{-3})	0.19, −0.23

Computer programs: *APEX3* and *SAINT* (Bruker, 2016), *SHELXT* (Sheldrick, 2015*a*), *SHELXL2018* (Sheldrick, 2015*b*), *DIAMOND* (Brandenburg & Putz, 2012) and *publCIF* (Westrip, 2010).

If the energy gap ΔE between the highest occupied molecular orbital (HOMO) and the lowest unoccupied molecular orbital (LUMO) is small, the molecule is highly polarizable and has high chemical reactivity. Numerical values of E_{HOMO} and E_{LUMO}, $\Delta E = E_{LUMO} - E_{HOMO}$, electronegativity ($\chi$), hardness ($\eta$), potential ($\mu$), electrophilicity ($\omega$) and softness ($\sigma$) for (I) are collated in Table 4. The significance of η and σ is to evaluate both the reactivity and stability. The shapes of the HOMO and the LUMO of molecule *A*, together with their energy levels are shown in Fig. 9.

6. Synthesis and crystallization

1,3-Dibromopropane (0.2 ml, 1.61 mmol) was added to a solution of eugenol (0.5 ml, 3.23 mmol), tetrabutylammonium chloride (50 mg) and sodium hydroxide solution (5%) in benzene as solvent (20 ml). The mixture was stirred at 293 K for 6 h, and then was extracted three times with dichloromethane (15 ml). The residue was purified by column chromatography on silica gel using a mixture of hexane/ethyl acetate (v/v = 97/3) as eluent. Colourless crystals were isolated when the solvent was allowed to evaporate (yield: 86%).

7. Refinement

Details including crystal data, data collection and refinement are summarized in Table 5. Hydrogen atoms were located in a difference-Fourier map and were refined freely.

Funding information

The support of NSF–MRI grant No. 1228232 for the purchase of the diffractometer and Tulane University for support of the Tulane Crystallography Laboratory are gratefully acknowledged. TH is grateful to Hacettepe University Scientific Research Project Unit (grant No. 013 D04 602 004). The Researchers Supporting Project (No. RSP-2019/78) King Saudi University, Riyadh, Saudi Arabia also supported this work.

References

Araújo, J. D. P., Grande, C. A. & Rodrigues, A. E. (2010). *Chem. Eng. Res. Des.* **88**, 1024–1032.
Becke, A. D. (1993). *J. Chem. Phys.* **98**, 5648–5652.
Brandenburg, K. & Putz, H. (2012). *DIAMOND*, Crystal Impact GbR, Bonn, Germany.
Bruker (2016). *APEX3* and *SAINT*. Bruker AXS, Inc., Madison, Wisconsin, USA.
Eyambe, G., Canales, L. & Banik, B. K. (2011). *Heterocyclic Lett.* **1**, 154–157.
Fonsêca, D. V., Salgado, P. R. R., Neto, H. C. A., Golzio, A. M. F. O., Caldas, M. R. D. F., Melo, C. G. F., Leite, F. C., Piuvezam, M. R., Pordeus, L. C. D., Barbosa, J. M. F. & Almeida, R. N. (2016). *Int. Immunopharmacol.* **38**, 402–408.
Frisch, M. J., Trucks, G. W., Schlegel, H. B., Scuseria, G. E., Robb, M. A., Cheeseman, J. R., *et al.* (2009). *GAUSSIAN09*. Gaussian Inc., Wallingford, CT, USA.
Ghosh, R., Nadiminty, N., Fitzpatrick, J. E., Alworth, W. L., Slaga, T. J. & Kumar, A. P. (2005). *J. Biol. Chem.* **280**, 5812–5819.
Hathwar, V. R., Sist, M., Jørgensen, M. R. V., Mamakhel, A. H., Wang, X., Hoffmann, C. M., Sugimoto, K., Overgaard, J. & Iversen, B. B. (2015). *IUCrJ*, **2**, 563–574.
Hirshfeld, H. L. (1977). *Theor. Chim. Acta*, **44**, 129–138.
Krause, L., Herbst-Irmer, R., Sheldrick, G. M. & Stalke, D. (2015). *J. Appl. Cryst.* **48**, 3–10.
Ma, Y.-T., Li, H.-Q., Shi, X.-W., Zhang, A.-L. & Gao, J.-M. (2010). *Acta Cryst.* E**66**, o2946.
Mahapatra, S. K., Chakraborty, S. P., Majumdar, S., Bag, B. G. & Roy, S. (2009). *Eur. J. Pharmacol.* **623**, 132–140.
McKinnon, J. J., Jayatilaka, D. & Spackman, M. A. (2007). *Chem. Commun.* pp. 3814–3816.
Morais, S. M. de, Vila-Nova, N. S., Bevilaqua, C. M. L., Rondon, F. C., Lobo, C. H., Moura, A. de A. A. N., Sales, A. D., Rodrigues, A. P. R., de Figuereido, J. R., Campello, C. C., Wilson, M. E. & de Andrade, H. F. (2014). *Bioorg. Med. Chem.* **22**, 6250–6255.
Nam, H. & Kim, M.-M. (2013). *Food & Chem. Toxicol.* **55**, 106–112.
Patra, A. K. & Saxena, J. (2010). *Phytochemistry*, **71**, 1198–1222.
Sadeghian, H., Seyedi, S. M., Saberi, M. R., Arghiani, Z. & Riazi, M. (2008). *Bioorg. Med. Chem.* **16**, 890–901.
Sheldrick, G. M. (2015*a*). *Acta Cryst.* A**71**, 3–8.
Sheldrick, G. M. (2015*b*). *Acta Cryst.* C**71**, 3–8.
Spackman, M. A. & Jayatilaka, D. (2009). *CrystEngComm*, **11**, 19–32.
Sticht, F. D. & Smith, R. M. (1971). *J. Dent. Res.* **50**, 1531–1535.
Sun, W. J., Lv, W. J., Li, L. N., Yin, G., Hang, X. F., Xue, Y. F., Chen, J. & Shi, Z. Q. (2016). *New Biotechnol.* **33**, 345–354.
Tiku, A. B., Abraham, S. K. & Kale, R. K. (2004). *J. Radiat. Res.* **45**, 435–440.
Turner, M. J., McKinnon, J. J., Wolff, S. K., Grimwood, D. J., Spackman, P. R., Jayatilaka, D. & Spackman, M. A. (2017). *CrystalExplorer17*. The University of Western Australia.
Venkatesan, P., Thamotharan, S., Ilangovan, A., Liang, H. & Sundius, T. (2016). *Spectrochim. Acta Part A*, **153**, 625–636.
Westrip, S. P. (2010). *J. Appl. Cryst.* **43**, 920–925.
Xu, H. X., Delling, M., Jun, J. C. & Clapham, D. E. (2006). *Nat. Neurosci.* **9**, 628–635.

supporting information

Acta Cryst. (2020). E**76**, 344-348 [https://doi.org/10.1107/S2056989020001681]

Crystal structure, Hirshfeld surface analysis and DFT studies of 1,3-bis[2-methoxy-4-(prop-2-en-1-yl)phenoxy]propane

Abdelmaoujoud Taia, Mohamed Essaber, Tuncer Hökelek, Abdeljalil Aatif, Joel T. Mague, Ali Alsalme and Nabil Al-Zaqri

Computing details

Data collection: *APEX3* (Bruker, 2016); cell refinement: *SAINT* (Bruker, 2016); data reduction: *SAINT* (Bruker, 2016); program(s) used to solve structure: *SHELXT* (Sheldrick, 2015*a*); program(s) used to refine structure: *SHELXL2018* (Sheldrick, 2015*b*); molecular graphics: *DIAMOND* (Brandenburg & Putz, 2012); software used to prepare material for publication: *publCIF* (Westrip, 2010).

1,3-Bis[2-methoxy-4-(prop-2-en-1-yl)phenoxy]propane

Crystal data

$C_{23}H_{28}O_4$
M_r = 368.45
Monoclinic, *P*2/*n*
a = 15.4741 (5) Å
b = 5.0224 (2) Å
c = 25.5180 (9) Å
β = 99.858 (2)°
V = 1953.90 (12) Å^3
Z = 4
F(000) = 792
D_x = 1.253 Mg m^{-3}
Cu *Kα* radiation, *λ* = 1.54178 Å
Cell parameters from 9361 reflections
θ = 3.5–72.4°
μ = 0.68 mm^{-1}
T = 150 K
Plate, colourless
0.37 × 0.27 × 0.08 mm

Data collection

Bruker D8 VENTURE PHOTON 100 CMOS diffractometer
Radiation source: INCOATEC I*μ*S micro–focus source
Mirror monochromator
Detector resolution: 10.4167 pixels mm^{-1}
ω scans
Absorption correction: multi-scan (*SADABS*; Krause *et al.*, 2015)
T_{min} = 0.79, T_{max} = 0.95
13935 measured reflections
3756 independent reflections
3049 reflections with $I > 2\sigma(I)$
R_{int} = 0.033
θ_{max} = 72.4°, θ_{min} = 3.1°
h = −19→18
k = −5→6
l = −31→29

Refinement

Refinement on F^2
Least-squares matrix: full
$R[F^2 > 2\sigma(F^2)]$ = 0.041
$wR(F^2)$ = 0.109
S = 1.05
3756 reflections
358 parameters
0 restraints
Primary atom site location: dual
Secondary atom site location: difference Fourier map
Hydrogen site location: difference Fourier map
All H-atom parameters refined
$w = 1/[\sigma^2(F_o^2) + (0.0537P)^2 + 0.5337P]$ where $P = (F_o^2 + 2F_c^2)/3$
$(\Delta/\sigma)_{max}$ = 0.001

$\Delta\rho_{max}$ = 0.19 e Å^{-3}
$\Delta\rho_{min}$ = −0.23 e Å^{-3}

Extinction correction: *SHELXL2018* (Sheldrick, 2015*b*), Fc*=kFc[1+0.001xFc$^{2}\lambda^{3}$/sin(2θ)]$^{-1/4}$
Extinction coefficient: 0.0071 (4)

Special details

Geometry. All esds (except the esd in the dihedral angle between two l.s. planes) are estimated using the full covariance matrix. The cell esds are taken into account individually in the estimation of esds in distances, angles and torsion angles; correlations between esds in cell parameters are only used when they are defined by crystal symmetry. An approximate (isotropic) treatment of cell esds is used for estimating esds involving l.s. planes.

Refinement. Refinement of F^2 against ALL reflections. The weighted R-factor wR and goodness of fit S are based on F^2, conventional R-factors R are based on F, with F set to zero for negative F^2. The threshold expression of $F^2 > 2\text{sigma}(F^2)$ is used only for calculating R-factors(gt) etc. and is not relevant to the choice of reflections for refinement. R-factors based on F^2 are statistically about twice as large as those based on F, and R- factors based on ALL data will be even larger.

Fractional atomic coordinates and isotropic or equivalent isotropic displacement parameters (Å^2)

	x	*y*	*z*	U_{iso}*/U_{eq}
O1	0.82230 (6)	−0.27068 (18)	0.30688 (3)	0.0222 (2)
O2	0.79368 (6)	0.06905 (18)	0.37794 (4)	0.0249 (2)
O3	0.32386 (6)	0.45366 (18)	0.30591 (3)	0.0223 (2)
O4	0.29863 (6)	0.12078 (19)	0.37925 (4)	0.0258 (2)
C1	0.89151 (8)	−0.1081 (2)	0.32631 (5)	0.0194 (3)
C2	0.87636 (8)	0.0744 (2)	0.36573 (5)	0.0203 (3)
C3	0.94260 (9)	0.2442 (3)	0.38859 (5)	0.0229 (3)
H3	0.9308 (10)	0.372 (3)	0.4158 (6)	0.026 (4)*
C4	1.02517 (8)	0.2399 (3)	0.37294 (5)	0.0227 (3)
C5	1.03861 (8)	0.0650 (3)	0.33324 (5)	0.0234 (3)
H5	1.0965 (11)	0.061 (3)	0.3204 (6)	0.028 (4)*
C6	0.97202 (8)	−0.1084 (3)	0.30986 (5)	0.0226 (3)
H6	0.9834 (10)	−0.232 (3)	0.2825 (6)	0.028 (4)*
C7	0.83297 (8)	−0.4437 (3)	0.26374 (5)	0.0219 (3)
H7A	0.8849 (10)	−0.562 (3)	0.2749 (6)	0.023 (4)*
H7B	0.8441 (10)	−0.334 (3)	0.2325 (6)	0.025 (4)*
C8	0.750000	−0.6078 (4)	0.250000	0.0224 (4)
H8B	0.7581 (11)	−0.722 (3)	0.2188 (6)	0.033 (4)*
C9	0.77076 (10)	0.2853 (3)	0.40922 (6)	0.0289 (3)
H9A	0.8027 (11)	0.277 (3)	0.4452 (7)	0.034 (4)*
H9B	0.7090 (11)	0.260 (3)	0.4097 (6)	0.028 (4)*
H9C	0.7809 (11)	0.458 (4)	0.3922 (7)	0.036 (4)*
C10	1.09695 (9)	0.4256 (3)	0.39847 (6)	0.0280 (3)
H10A	1.1474 (11)	0.420 (3)	0.3779 (6)	0.035 (4)*
H10B	1.0731 (12)	0.613 (4)	0.3959 (7)	0.040 (5)*
C11	1.13272 (9)	0.3754 (3)	0.45635 (6)	0.0298 (3)
H11	1.1823 (13)	0.494 (4)	0.4714 (7)	0.052 (5)*
C12	1.10801 (11)	0.1937 (3)	0.48750 (6)	0.0355 (4)
H12A	1.1352 (12)	0.181 (4)	0.5248 (7)	0.044 (5)*
H12B	1.0621 (13)	0.067 (4)	0.4757 (7)	0.047 (5)*
C13	0.39264 (8)	0.2882 (2)	0.32379 (5)	0.0198 (3)
C14	0.37979 (8)	0.1110 (2)	0.36473 (5)	0.0204 (3)

C15	0.44651 (9)	−0.0598 (3)	0.38657 (5)	0.0230 (3)
H15	0.4371 (11)	−0.180 (3)	0.4150 (6)	0.032 (4)*
C16	0.52658 (8)	−0.0646 (3)	0.36808 (5)	0.0229 (3)
C17	0.53771 (8)	0.1037 (3)	0.32686 (5)	0.0235 (3)
H17	0.5958 (10)	0.104 (3)	0.3123 (6)	0.026 (4)*
C18	0.47108 (8)	0.2800 (3)	0.30487 (5)	0.0224 (3)
H18	0.4801 (10)	0.400 (3)	0.2759 (6)	0.023 (4)*
C19	0.33292 (8)	0.6261 (3)	0.26230 (5)	0.0213 (3)
H19A	0.3426 (10)	0.514 (3)	0.2309 (6)	0.023 (4)*
H19B	0.3849 (10)	0.743 (3)	0.2722 (6)	0.026 (4)*
C20	0.250000	0.7913 (4)	0.250000	0.0223 (4)
H20B	0.2441 (11)	0.908 (3)	0.2806 (6)	0.031 (4)*
C21	0.27648 (10)	−0.0984 (3)	0.41011 (6)	0.0289 (3)
H21A	0.2830 (11)	−0.273 (3)	0.3913 (6)	0.034 (4)*
H21B	0.2159 (12)	−0.073 (3)	0.4127 (6)	0.036 (4)*
H21C	0.3109 (11)	−0.096 (3)	0.4452 (7)	0.033 (4)*
C22	0.59762 (9)	−0.2578 (3)	0.39229 (6)	0.0275 (3)
H22A	0.5774 (11)	−0.442 (4)	0.3845 (7)	0.037 (4)*
H22B	0.6510 (11)	−0.225 (3)	0.3753 (6)	0.034 (4)*
C23	0.62171 (9)	−0.2341 (3)	0.45158 (6)	0.0300 (3)
H23	0.6524 (13)	−0.064 (4)	0.4645 (7)	0.050 (5)*
C24	0.60596 (11)	−0.4141 (3)	0.48616 (7)	0.0386 (4)
H24A	0.5776 (13)	−0.581 (4)	0.4740 (8)	0.051 (5)*
H24B	0.6230 (13)	−0.389 (4)	0.5240 (8)	0.050 (5)*

Atomic displacement parameters (Å²)

	U^{11}	U^{22}	U^{33}	U^{12}	U^{13}	U^{23}
O1	0.0208 (4)	0.0227 (5)	0.0230 (5)	−0.0028 (4)	0.0034 (3)	−0.0050 (4)
O2	0.0209 (5)	0.0269 (5)	0.0276 (5)	0.0002 (4)	0.0063 (4)	−0.0056 (4)
O3	0.0212 (4)	0.0223 (5)	0.0232 (5)	0.0035 (4)	0.0032 (3)	0.0049 (4)
O4	0.0225 (5)	0.0274 (5)	0.0289 (5)	0.0031 (4)	0.0084 (4)	0.0061 (4)
C1	0.0191 (6)	0.0183 (6)	0.0197 (6)	−0.0008 (5)	0.0002 (5)	0.0022 (5)
C2	0.0200 (6)	0.0215 (6)	0.0193 (6)	0.0012 (5)	0.0031 (5)	0.0022 (5)
C3	0.0256 (7)	0.0208 (6)	0.0213 (6)	0.0009 (5)	0.0010 (5)	−0.0006 (5)
C4	0.0221 (6)	0.0215 (6)	0.0224 (6)	−0.0019 (5)	−0.0015 (5)	0.0046 (5)
C5	0.0196 (6)	0.0265 (7)	0.0240 (6)	−0.0004 (5)	0.0033 (5)	0.0045 (6)
C6	0.0238 (6)	0.0224 (6)	0.0216 (6)	0.0016 (5)	0.0041 (5)	0.0002 (5)
C7	0.0238 (7)	0.0203 (6)	0.0209 (6)	0.0012 (5)	0.0023 (5)	−0.0026 (5)
C8	0.0247 (9)	0.0188 (8)	0.0223 (9)	0.000	0.0001 (7)	0.000
C9	0.0293 (7)	0.0278 (7)	0.0314 (8)	0.0045 (6)	0.0100 (6)	−0.0045 (6)
C10	0.0265 (7)	0.0263 (7)	0.0293 (7)	−0.0065 (6)	−0.0006 (6)	0.0028 (6)
C11	0.0276 (7)	0.0308 (7)	0.0285 (7)	−0.0026 (6)	−0.0015 (5)	−0.0040 (6)
C12	0.0367 (8)	0.0419 (9)	0.0258 (8)	−0.0008 (7)	−0.0007 (6)	0.0021 (7)
C13	0.0207 (6)	0.0174 (6)	0.0199 (6)	0.0013 (5)	0.0000 (5)	−0.0022 (5)
C14	0.0197 (6)	0.0210 (6)	0.0203 (6)	−0.0007 (5)	0.0033 (5)	−0.0027 (5)
C15	0.0248 (6)	0.0221 (6)	0.0212 (6)	0.0019 (5)	0.0013 (5)	0.0013 (5)
C16	0.0227 (6)	0.0219 (6)	0.0222 (6)	0.0013 (5)	−0.0015 (5)	−0.0052 (5)

C17	0.0209 (6)	0.0240 (6)	0.0254 (7)	−0.0008 (5)	0.0032 (5)	−0.0048 (5)
C18	0.0227 (6)	0.0217 (6)	0.0225 (6)	−0.0020 (5)	0.0033 (5)	−0.0004 (5)
C19	0.0226 (6)	0.0204 (6)	0.0206 (6)	−0.0004 (5)	0.0026 (5)	0.0027 (5)
C20	0.0249 (9)	0.0181 (8)	0.0224 (9)	0.000	0.0001 (7)	0.000
C21	0.0297 (7)	0.0280 (7)	0.0308 (8)	−0.0009 (6)	0.0104 (6)	0.0053 (6)
C22	0.0253 (7)	0.0252 (7)	0.0295 (7)	0.0055 (6)	−0.0019 (5)	−0.0036 (6)
C23	0.0282 (7)	0.0280 (7)	0.0311 (7)	0.0040 (6)	−0.0029 (6)	0.0007 (6)
C24	0.0411 (9)	0.0364 (9)	0.0381 (9)	0.0078 (7)	0.0059 (7)	0.0063 (7)

Geometric parameters (Å, º)

O1—C1	1.3704 (15)	C11—C12	1.310 (2)
O1—C7	1.4342 (15)	C11—H11	0.99 (2)
O2—C2	1.3679 (15)	C12—H12A	0.975 (19)
O2—C9	1.4280 (16)	C12—H12B	0.96 (2)
O3—C13	1.3658 (15)	C13—C18	1.3816 (18)
O3—C19	1.4359 (15)	C13—C14	1.4121 (17)
O4—C14	1.3697 (15)	C14—C15	1.3840 (18)
O4—C21	1.4289 (16)	C15—C16	1.3995 (18)
C1—C6	1.3812 (18)	C15—H15	0.974 (17)
C1—C2	1.4098 (17)	C16—C17	1.3828 (19)
C2—C3	1.3831 (19)	C16—C22	1.5162 (18)
C3—C4	1.4025 (18)	C17—C18	1.4015 (19)
C3—H3	0.984 (16)	C17—H17	1.030 (15)
C4—C5	1.3833 (19)	C18—H18	0.984 (16)
C4—C10	1.5099 (18)	C19—C20	1.5148 (16)
C5—C6	1.4021 (19)	C19—H19A	1.012 (15)
C5—H5	1.005 (16)	C19—H19B	0.992 (16)
C6—H6	0.972 (16)	C20—H20B	0.993 (16)
C7—C8	1.5154 (16)	C20—H20B^{ii}	0.993 (16)
C7—H7A	1.003 (16)	C21—H21A	1.013 (17)
C7—H7B	1.007 (15)	C21—H21B	0.960 (18)
C8—H8B	1.007 (16)	C21—H21C	0.961 (17)
C8—H8B^{i}	1.007 (16)	C22—C23	1.499 (2)
C9—H9A	0.967 (17)	C22—H22A	0.984 (18)
C9—H9B	0.966 (17)	C22—H22B	1.010 (17)
C9—H9C	0.993 (18)	C23—C24	1.315 (2)
C10—C11	1.507 (2)	C23—H23	1.00 (2)
C10—H10A	1.014 (17)	C24—H24A	0.97 (2)
C10—H10B	1.008 (18)	C24—H24B	0.97 (2)
O1···O2	2.5827 (13)	C14···H20B^{iii}	2.918 (15)
O2···O1	2.5827 (13)	C15···H21A	2.768 (17)
O3···O4	2.5885 (13)	C15···H21C	2.784 (17)
O4···O3	2.5885 (13)	C17···H22A^{vi}	2.727 (19)
O1···H9C^{iii}	2.736 (18)	C18···H22A^{vi}	2.764 (18)
O1···H7B^{i}	2.618 (16)	C18···H19A	2.759 (15)
O2···H12A^{iv}	2.831 (18)	C18···H19B	2.739 (15)

O2···H22B	2.647 (17)	C19···H18	2.514 (16)
O2···H8B^{v}	2.676 (15)	C21···H15	2.501 (16)
O3···H21A^{vi}	2.739 (15)	C23···H15	2.862 (16)
O3···H19A^{ii}	2.604 (16)	H3···H9C	2.33 (2)
O4···H24B^{vii}	2.89 (2)	H3···H9A	2.29 (2)
O4···H20B^{iii}	2.732 (15)	H5···H10A	2.37 (2)
C2···C7^{vi}	3.533 (2)	H6···H7A	2.24 (2)
C3···C12	3.282 (2)	H6···H7B	2.37 (2)
C6···C10^{iii}	3.582 (2)	H6···H18^{viii}	2.50 (2)
C14···C19^{iii}	3.555 (2)	H9A···H11^{ix}	2.40 (2)
C18···C22^{vi}	3.564 (2)	H9A···H12A^{iv}	2.56 (3)
C2···H8B^{v}	2.914 (16)	H9B···H22A^{vi}	2.52 (2)
C2···H7A^{vi}	2.971 (15)	H9B···H23	2.41 (2)
C3···H9C	2.739 (18)	H9C···H22B^{vi}	2.54 (2)
C3···H12B	2.783 (19)	H10A···H21A^{x}	2.58 (2)
C3···H9A	2.806 (17)	H12B···H12B^{iv}	2.55 (3)
C4···H12B	2.728 (18)	H15···H21A	2.40 (2)
C5···H10B^{iii}	2.775 (19)	H15···H21C	2.26 (2)
C6···H7A	2.719 (15)	H17···H22B	2.36 (2)
C6···H7B	2.786 (15)	H18···H19A	2.31 (2)
C6···H10B^{iii}	2.837 (18)	H18···H19B	2.26 (2)
C7···H6	2.529 (16)	H21C···H23^{vii}	2.41 (2)
C9···H3	2.492 (16)	H22A···H24A	2.39 (3)

C1—O1—C7	116.96 (10)	C11—C12—H12B	123.1 (11)
C2—O2—C9	116.34 (10)	H12A—C12—H12B	115.9 (15)
C13—O3—C19	116.88 (10)	O3—C13—C18	125.61 (11)
C14—O4—C21	116.03 (10)	O3—C13—C14	115.48 (11)
O1—C1—C6	125.38 (11)	C18—C13—C14	118.90 (11)
O1—C1—C2	115.50 (11)	O4—C14—C15	124.66 (12)
C6—C1—C2	119.12 (11)	O4—C14—C13	115.42 (11)
O2—C2—C3	124.79 (12)	C15—C14—C13	119.91 (12)
O2—C2—C1	115.21 (11)	C14—C15—C16	121.15 (12)
C3—C2—C1	119.99 (12)	C14—C15—H15	119.3 (10)
C2—C3—C4	121.06 (12)	C16—C15—H15	119.6 (10)
C2—C3—H3	119.0 (9)	C17—C16—C15	118.61 (12)
C4—C3—H3	119.9 (9)	C17—C16—C22	121.67 (12)
C5—C4—C3	118.47 (12)	C15—C16—C22	119.70 (12)
C5—C4—C10	121.09 (12)	C16—C17—C18	120.79 (12)
C3—C4—C10	120.43 (12)	C16—C17—H17	120.3 (8)
C4—C5—C6	120.97 (12)	C18—C17—H17	118.9 (9)
C4—C5—H5	120.3 (9)	C13—C18—C17	120.59 (12)
C6—C5—H5	118.7 (9)	C13—C18—H18	119.4 (9)
C1—C6—C5	120.34 (12)	C17—C18—H18	120.0 (9)
C1—C6—H6	120.2 (9)	O3—C19—C20	107.42 (9)
C5—C6—H6	119.4 (9)	O3—C19—H19A	109.0 (9)
O1—C7—C8	107.63 (9)	C20—C19—H19A	112.1 (8)
O1—C7—H7A	109.5 (8)	O3—C19—H19B	109.9 (9)

C8—C7—H7A	110.4 (9)	C20—C19—H19B	110.6 (9)
O1—C7—H7B	109.4 (9)	H19A—C19—H19B	107.9 (12)
C8—C7—H7B	111.6 (9)	C19—C20—C19^{ii}	113.61 (15)
H7A—C7—H7B	108.2 (12)	C19—C20—H20B	110.4 (9)
C7—C8—C7^{i}	114.11 (15)	C19^{ii}—C20—H20B	107.3 (9)
C7—C8—H8B	106.1 (9)	C19—C20—H20B^{ii}	107.3 (9)
C7^{i}—C8—H8B	110.0 (9)	C19^{ii}—C20—H20B^{ii}	110.4 (9)
C7—C8—H8B^{i}	110.0 (9)	H20B—C20—H20B^{ii}	107.6 (18)
C7^{i}—C8—H8B^{i}	106.1 (9)	O4—C21—H21A	110.7 (9)
H8B—C8—H8B^{i}	110.5 (18)	O4—C21—H21B	105.3 (10)
O2—C9—H9A	111.2 (10)	H21A—C21—H21B	109.0 (14)
O2—C9—H9B	104.5 (9)	O4—C21—H21C	111.0 (10)
H9A—C9—H9B	109.1 (13)	H21A—C21—H21C	111.5 (14)
O2—C9—H9C	110.3 (10)	H21B—C21—H21C	109.1 (13)
H9A—C9—H9C	111.2 (14)	C23—C22—C16	113.46 (11)
H9B—C9—H9C	110.5 (13)	C23—C22—H22A	107.1 (10)
C11—C10—C4	116.06 (12)	C16—C22—H22A	109.6 (10)
C11—C10—H10A	108.5 (9)	C23—C22—H22B	109.9 (9)
C4—C10—H10A	109.5 (10)	C16—C22—H22B	108.1 (10)
C11—C10—H10B	106.7 (10)	H22A—C22—H22B	108.7 (14)
C4—C10—H10B	108.3 (10)	C24—C23—C22	125.43 (15)
H10A—C10—H10B	107.5 (14)	C24—C23—H23	119.7 (11)
C12—C11—C10	127.94 (14)	C22—C23—H23	114.8 (11)
C12—C11—H11	118.0 (11)	C23—C24—H24A	120.3 (11)
C10—C11—H11	114.0 (11)	C23—C24—H24B	122.2 (12)
C11—C12—H12A	121.0 (11)	H24A—C24—H24B	117.5 (17)

C7—O1—C1—C6	−3.97 (17)	C19—O3—C13—C18	2.61 (18)
C7—O1—C1—C2	175.08 (10)	C19—O3—C13—C14	−176.67 (10)
C9—O2—C2—C3	11.70 (18)	C21—O4—C14—C15	−14.30 (18)
C9—O2—C2—C1	−167.55 (11)	C21—O4—C14—C13	164.57 (11)
O1—C1—C2—O2	−1.88 (16)	O3—C13—C14—O4	2.86 (16)
C6—C1—C2—O2	177.24 (11)	C18—C13—C14—O4	−176.47 (11)
O1—C1—C2—C3	178.83 (11)	O3—C13—C14—C15	−178.22 (11)
C6—C1—C2—C3	−2.05 (18)	C18—C13—C14—C15	2.45 (18)
O2—C2—C3—C4	−178.74 (12)	O4—C14—C15—C16	177.52 (12)
C1—C2—C3—C4	0.48 (19)	C13—C14—C15—C16	−1.29 (19)
C2—C3—C4—C5	1.21 (19)	C14—C15—C16—C17	−0.69 (19)
C2—C3—C4—C10	−179.70 (12)	C14—C15—C16—C22	−178.93 (12)
C3—C4—C5—C6	−1.35 (19)	C15—C16—C17—C18	1.52 (19)
C10—C4—C5—C6	179.57 (12)	C22—C16—C17—C18	179.71 (12)
O1—C1—C6—C5	−179.06 (11)	O3—C13—C18—C17	179.10 (12)
C2—C1—C6—C5	1.92 (19)	C14—C13—C18—C17	−1.65 (19)
C4—C5—C6—C1	−0.22 (19)	C16—C17—C18—C13	−0.34 (19)
C1—O1—C7—C8	178.57 (10)	C13—O3—C19—C20	−179.34 (10)
O1—C7—C8—C7^{i}	56.52 (7)	O3—C19—C20—C19^{ii}	−56.61 (7)
C5—C4—C10—C11	−113.66 (15)	C17—C16—C22—C23	126.83 (14)

C3—C4—C10—C11	67.28 (17)	C15—C16—C22—C23	−55.00 (17)
C4—C10—C11—C12	−1.4 (2)	C16—C22—C23—C24	111.83 (17)

Symmetry codes: (i) −*x*+3/2, *y*, −*z*+1/2; (ii) −*x*+1/2, *y*, −*z*+1/2; (iii) *x*, *y*−1, *z*; (iv) −*x*+2, −*y*, −*z*+1; (v) −*x*+3/2, *y*+1, −*z*+1/2; (vi) *x*, *y*+1, *z*; (vii) −*x*+1, −*y*, −*z*+1; (viii) −*x*+3/2, *y*−1, −*z*+1/2; (ix) −*x*+2, −*y*+1, −*z*+1; (x) *x*+1, *y*+1, *z*.

Hydrogen-bond geometry (Å, º)

*Cg*1 and *Cg*2 are the centroids of benzene rings *A* (C1–C6) and *B* (C13–C18), respectively.

D—H···*A*	*D*—H	H···*A*	*D*···*A*	*D*—H···*A*
C7—H7*A*···*Cg*1^{iii}	1.003 (16)	2.759 (15)	3.6170 (15)	144.1 (12)
C19—H19*B*···*Cg*2^{vi}	0.992 (16)	2.739 (15)	3.5816 (15)	143.0 (11)

Symmetry codes: (iii) *x*, *y*−1, *z*; (vi) *x*, *y*+1, *z*.